

Locally Optimal PI Controller for a Two-Tank System

Igor Krčmar, Velibor Đalić, Aleksandar Rakić, and Petar Marić

Abstract— The paper provides an extensive experimental analysis of an optimal PI controller for the two-tank system. The two-tank system is a benchmark hydrodynamic system. The PI controller has proportional action placed in a feedback path of the system, thus supporting aperiodic response of the system. The optimal PI controller tuning is based on transfer function of the system, and it minimizes surface between the error signal and the time axis. The choice of the minimization criterion is adequate as the system has aperiodic step response. The extensive experimental analysis is performed on the laboratory testbed to assess the performance of the optimally tuned PI controller when applied to the two-tank systems in step response tasks, reference tracking tasks, and disturbance rejection tasks. The results of the experiments verify the design procedure of the PI controller. The designed PI controller provides noticeable slow start of the system, thus forcing an actuator to operate on a border line of the dead zone for a significant period. To remedy the situation, a feedforward modification of the controller is proposed. Gain of the feedforward part is time varying. At the beginning of the system operation, it provides significant value of the control signal and safe start of the system. On the other hand, as time advances, the gain of the feedforward part vanishes to zero. Although the feedforward modification detunes optimal behavior of the system, it adds value to the operation of the system. Experimental analysis performed on the laboratory testbed verifies utilities introduced by the feedforward controller modification.

Index Terms— experimental analysis, optimization procedure, proportional and integral controller, two-tank system, feedforward controller.

Paper Classification
DOI: 10.53314/ELS2428068K

Manuscript received on December 1st, 2024. Received in revised form on December 20th and 24th, 2024. Accepted for publication on December 25th, 2024.

Igor Krčmar is with the Faculty of Electrical Engineering, University of Banja Luka, Banja Luka, Bosnia and Herzegovina (phone: +387-51-221-820; e-mail: igor.krčmar@etf.unibl.org).

Velibor Đalić is with the Faculty of Electrical Engineering, University of Banja Luka, Banja Luka, Bosnia and Herzegovina (e-mail: velibor.djalic@etf.unibl.org).

Aleksandar Rakić is with the School of Electrical Engineering, University of Belgrade, Belgrade, Serbia (e-mail: rakic@etf.rs).

Petar Marić is with the Faculty of Electrical Engineering, University of Banja Luka, Banja Luka, Bosnia and Herzegovina (e-mail: petar.marić@etf.unibl.org).

I. INTRODUCTION

Coupled tanks systems are part of industrial facilities, urban infrastructure, and water supply systems [1], [2]. Modern human society suffers from lack of resources and/or their uneven distribution, such as energy and drinking water [3], [1]. Therefore, some regions and countries organize water supply services on market principles, which requires adequate measurement and control of provided service, on all levels [4], [3]. Coupled tanks systems implement a hydrodynamic process, i. e. liquid flow and storage process [5]. The hydrodynamic process is nonlinear and has significant inertia, even when implemented as laboratory setup [6], [7], [5]. The DTS 200 laboratory setup [8], configured as the two-tank system, can exhibit very complex dynamical behavior [9]. Thus, it is considered as a benchmark hydrodynamic system. Control of such a system might be a very challenging task, with limited resources for implementation. So, it must be simple, yet efficient.

The proportional, integral, and derivative (PID) controller is very simple, with three adjustable parameters, and clear physical interpretation [10], [11]. Due to its simplicity and efficiency, the PID controller has gained significant popularity which resulted in numerous applications [12]. There are applications where the proportional and integral (PI) controller can provide desired dynamical behavior and steady state accuracy [10], [11], [12].

Performance of the PI and the PID controllers can be improved through an optimization of tuning procedure [13], [14], [15]. In the case of systems with aperiodic step response, error signal does not change sign, thus integral error (IE) can be used as a criterion function for the optimal PI controller tuning [16], [10].

Recently, optimal PI controller for the two-tank system was proposed [17]. It defines tuning of the PI controller parameters as the optimization procedure, which adopts minimization of IE as criterion. The proposed controller has modified structure, i. e. proportional action of the controller is placed in a feedback path. Modification was implemented to support aperiodic step response of the system. The optimal PI controller tuning is based on a transfer function of the system. Thus, it is locally optimal. The benchmark two-tank system [8] is a nonlinear system [6], [7], [8], [9]. Therefore, the transfer function of the system depends on the choice of an operational point.

Thus, the aim of this paper is to examine and assess the performance of the proposed optimal PI controller through extensive experimental analysis. The experimental analysis is performed on the two-tank system realized by the DTS 200 laboratory setup [8]. In addition, a feedforward modification is introduced in the system structure to improve the start of the system operation. Applied methodology intends to provide self-contained and easy to follow material, thus it provides derivation of optimally tuned PI controller as given in [17].

Therefore, the organization of the paper is as follows. Section II provides mathematical modelling of the two-tank system. The model is provided as the transfer function of the system. Section III presents derivation of the optimal PI controller tuning procedure. Section IV gives the experimental analysis. It contains system identification, step response experiments, reference tracking experiments, and disturbance rejection experiments, as well as comparison of the proposed PI controller with PI and PID controllers tuned according to the Ziegler-Nichols procedure. Section V presents feedforward modification of the controller, while concluding remarks and ideas for future work are presented in Section VI. At the end of the paper, a list of used references is given.

II. MATHEMATICAL MODELLING OF THE SYSTEM

The structure of the system under consideration is presented in Fig. 1. Mathematical model is derived following principles and procedures given in [5], [8], [17]. The two-tank system has two accumulators of masses, i. e. tanks T_1 and T_2 . Mathematical modelling starts with equations of dynamical equilibria for each tank. These equations are

$$\dot{M}_1(t) = m_{in}(t) - m_{12}(t), \quad (1)$$

$$\dot{M}_2(t) = m_{12}(t) - m_{out}(t), \quad (2)$$

where M_1 and M_2 denote water masses stored in tanks T_1 and T_2 , respectively, m_{in} is input mass flow, m_{out} is output mass flow, m_{12} denotes mass flow between the tanks, t denotes time and $(\dot{\cdot})$ is the first derivative.

The tanks are, constructively, cylinders with constant surface of the cross-section, denoted with S . Therefore, masses stored in tanks are given with the following equations

$$M_1(t) = \rho V_1(t) = \rho S H_1(t), \quad (3)$$

$$M_2(t) = \rho V_2(t) = \rho S H_2(t), \quad (4)$$

where V_1 and V_2 denote volumes of the water stored in tanks T_1 and T_2 , respectively, H_1 and H_2 denote levels of the water stored in T_1 and T_2 , respectively and ρ is water density. Mass flows are defined as follows

$$m_{out}(t) = K_{out} A_{out} \rho \sqrt{2g H_2(t)}, \quad (5)$$

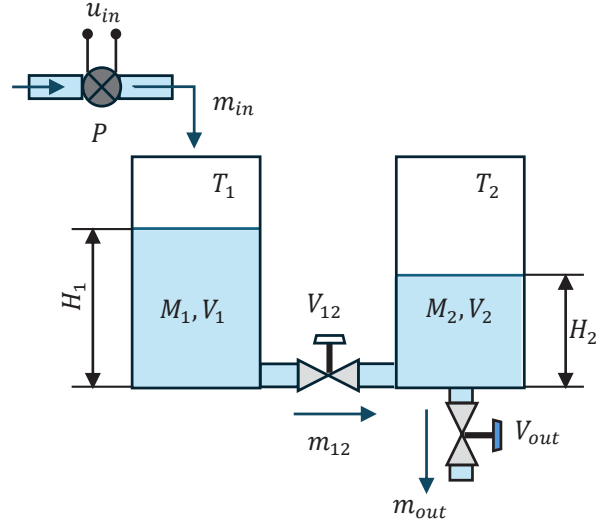


Fig. 1. Structure of the two-tank system with key elements and physical quantities presented

$$m_{12}(t) = K_{12} A_{12} \rho \sqrt{2g [H_1(t) - H_2(t)]}, \quad (6)$$

$$m_{in}(t) = K_a u_{in}(t). \quad (7)$$

In (5), K_{out} denotes constant of the valve V_{out} , A_{out} is surface of, so called, light cross-section of the valve V_{out} and g denotes the gravity of Earth. In (6), K_{12} denotes constant of the valve V_{12} and A_{12} is surface of light cross-section of the valve V_{12} . Model of the actuator, i. e. pump denoted by P in Fig. 1., is given by (7). The actuator is modeled as a system with no inertia when compared to the dynamics of water flow and storage process [5], [8], [17]. In (7), u_{in} denotes input voltage to the actuator and K_a is slope of the static characteristic of the actuator, determined at the linear portion of the characteristic [17]. Combining equations (1) – (7) the following holds

$$\begin{aligned} \dot{H}_1(t) &= (K_a / \rho S) u_{in}(t) - \\ & (K_{12} A_{12} / S) \sqrt{2g [H_1(t) - H_2(t)]} = K_a^* u_{in}(t) - \\ & K_{12}^* \sqrt{[H_1(t) - H_2(t)]}, \end{aligned} \quad (8)$$

$$\begin{aligned} \dot{H}_2(t) &= (K_{12} A_{12} / S) \sqrt{2g [H_1(t) - H_2(t)]} - \\ & (K_{out} A_{out} / S) \sqrt{2g H_2(t)} = K_{12}^* \sqrt{[H_1(t) - H_2(t)]} \\ & - K_{out}^* \sqrt{H_2(t)}. \end{aligned} \quad (9)$$

Bearing in mind the structure of the system, given in Fig. 1., it is obvious that there is water flow in one direction only, from the input to the output. This means that tank T_1 supplies water for T_2 , thus $H_1(t) \geq H_2(t)$. Also, input voltage u_{in} is unipolar. If $H_2(t)$ is adopted as the output of the system and $x(t) = [H_1(t) \ H_2(t)]^T$, $[\cdot]^T$ denotes vector transpose, is introduced as state vector, model of the system can be given in vector form

$$\dot{x}(t) = f(x, u) = [f_1(x, u) \ f_2(x, u)]^T, \quad (10)$$

$$y(t) = g(x, u) = [0 \ 1]x(t) = H_2(t), \quad (11)$$

where system input is $u(t) = u_{in}(t)$. To obtain a model of the system in the form of transfer function, linearization of the nonlinear model given by (8) and (9), i. e. (10) and (11). Linearization of the nonlinear model will be performed in a vicinity of a steady state. The system is driven to the steady state by $u(t) = u_{in}(t) = u_{in,ss}$. The steady state is defined by the following relationship

$$\dot{x}(t) = 0. \quad (12)$$

Relationship (12) yields the following equations

$$\dot{H}_1(t) = K_a^* u_{in,ss} - K_{12}^* \sqrt{[H_1(t) - H_2(t)]} = 0, \quad (13)$$

$$\dot{H}_2(t) = K_{12}^* \sqrt{[H_1(t) - H_2(t)]} - K_{out}^* \sqrt{H_2(t)} = 0. \quad (14)$$

From (13) and (14), the following holds

$$K_a^* u_{in,ss} = K_{12}^* \sqrt{H_{1,ss} - H_{2,ss}}, \quad (15)$$

$$K_{12}^* \sqrt{H_{1,ss} - H_{2,ss}} = K_{out}^* \sqrt{H_{2,ss}}, \quad (16)$$

where $H_{1,ss}$ and $H_{2,ss}$ denote steady state water levels in T_1 and T_2 , respectively. Values of K_{12}^* and K_{out}^* follows from (15) and (16) as

$$K_{12}^* = K_a^* u_{in,ss} / \sqrt{H_{1,ss} - H_{2,ss}}, \quad (17)$$

$$K_{out}^* = K_a^* u_{in,ss} / \sqrt{H_{2,ss}}. \quad (18)$$

Linearized model is given by [18], [5], [17]

$$\Delta \dot{x}(t) = \begin{bmatrix} \partial f_1 / \partial H_1 & \partial f_1 / \partial H_2 \\ \partial f_2 / \partial H_1 & \partial f_2 / \partial H_2 \end{bmatrix}_{ss} \Delta x(t) + \begin{bmatrix} \partial f_1 / \partial u_{in} \\ \partial f_2 / \partial u_{in} \end{bmatrix}_{ss} \Delta u(t), \quad (19)$$

$$\Delta y(t) = [0 \ 1] \Delta x(t) = H \Delta x(t) = \Delta H_2(t). \quad (20)$$

Subscript "ss" in (19) denotes that partial derivatives are computed at the steady state. Further, $\Delta x(t) = x(t) - x_{ss} = [\Delta H_1(t) \ \Delta H_2(t)]^T = [H_1(t) - H_{1,ss} \ H_2(t) - H_{2,ss}]^T$ and $\Delta u(t) = u_{in}(t) - u_{in,ss}$. Computation of partial derivatives in (19) gives matrices

$$F_x = \begin{bmatrix} \partial f_1 / \partial H_1 & \partial f_1 / \partial H_2 \\ \partial f_2 / \partial H_1 & \partial f_2 / \partial H_2 \end{bmatrix}_{ss} = \begin{bmatrix} -K_a^* u_{in,ss} & K_a^* u_{in,ss} \\ \frac{2(H_{1,ss} - H_{2,ss})}{K_a^* u_{in,ss}} & \frac{2(H_{1,ss} - H_{2,ss})}{-K_a^* u_{in,ss} - \frac{K_a^* u_{in,ss}}{2H_{2,ss}}} \end{bmatrix} = \begin{bmatrix} -a & a \\ a & -b \end{bmatrix}, \quad (21)$$

$$F_u = \begin{bmatrix} \partial f_1 / \partial u_{in} \\ \partial f_2 / \partial u_{in} \end{bmatrix}_{ss} = \begin{bmatrix} K_a^* \\ 0 \end{bmatrix}. \quad (22)$$

Now, linearized model of the system can be written as

$$\Delta \dot{x}(t) = F_x \Delta x(t) + F_u \Delta u(t), \quad (23)$$

$$\Delta y(t) = F_y \Delta x(t). \quad (24)$$

Application of Laplace transform to (23) and (24), under assumption of zero initial conditions, yields [19]

$$sX(s) = F_x X(s) + F_u U(s), \quad (25)$$

$$Y(s) = F_y X(s), \quad (26)$$

where symbol Δ is omitted for simpler notation, keeping in mind proper interpretation, s is complex variable, $X(s) = \mathcal{L}[x(t)]$, $U(s) = \mathcal{L}[u(t)]$, $Y(s) = \mathcal{L}[y(t)]$, and $\mathcal{L}[\cdot]$ denotes Laplace transform. Now, from (25) and (26), transfer function of the system is given by

$$G_{tts}(s) = Y(s)/U(s) = F_y (sI - F_x)^{-1} F_u, \quad (27)$$

where I is unitary matrix of appropriate dimension and $(\cdot)^{-1}$ denotes matrix inversion. Introduction of (21) and (22) to (27) yields

$$G_{tts}(s) = a K_a^* / [s^2 + s(a+b) + ab - a^2]. \quad (28)$$

Solving equation $s^2 + s(a+b) + ab - a^2 = 0$ gives poles of the transfer function

$$p_{1,2} = -(a+b)/2 \pm (1/2) \sqrt{(a+b)^2 - 4(ab - a^2)} \\ = -(a+b)/2 \pm (1/2) \sqrt{(a-b)^2 + 4a^2}. \quad (29)$$

From (21), it follows $b > a$. Now, (29) with $b > a$ yields $p_1, p_2 \in \mathbb{R}$, \mathbb{R} is set of real numbers, and $p_1, p_2 < 0$. It can be concluded, in the neighborhood of steady state, the two-tank system can be modeled with transfer function

$$G_{tts}(s) = K / [(s - p_1)(s - p_2)]. \quad (30)$$

The transfer function describes stable second order system, with two real poles and no finite zeros.

III. DESIGN OF OPTIMAL PI CONTROLLER

The design of PI controller, in a certain way, follows optimization procedure derived in [17]. The main goal of the design procedure is to obtain fast aperiodic step response of the system. In the case of an aperiodic system step response, error signal defined as

$$e(t) = r(t) - y(t), \quad (31)$$

where $r(t)$ is reference signal and $y(t)$ is output signal, does not change sign. If $r(t) = h(t)$, where $h(t)$ denotes Heaviside signal, $e(t)$ is positive, or at least nonnegative for all $t \geq 0$. Therefore, the following criterion is adopted

$$J_{IE} = \int_0^{\infty} e(t) dt. \quad (32)$$

Minimization of the criterion (32) will yield optimal values of the parameters of PI controller. The structure of the overall system is presented in Fig. 2. The integral action of the controller is in the direct path, while the proportional action of the controller is placed in a feedback path, i. e. it acts only on the output signal. This is done to avoid an overshoot in the step response of the system.

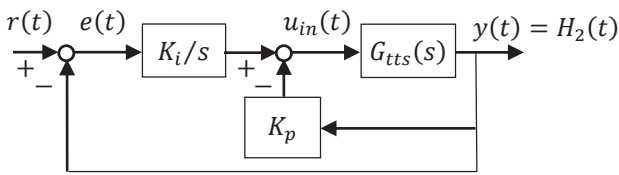


Fig. 2. Block diagram of the system with the proposed PI controller, K_p is in the feedback path

State space model of the system given in Fig. 2. can be built upon the model given by (21), (22), (23), and (24). To that cause, it should be noted that integral action of the PI controller adds a state variable to the model. If new state variable is denoted by x_3 , it follows from Fig. 2. That

$$\dot{x}_3(t) = e(t), \quad (33)$$

$$u(t) = K_i x_3(t) - K_p y(t). \quad (34)$$

Again, symbol Δ is omitted for the sake of simplicity. Also, it should be stressed that $x_3(t) = \int_0^t e(\tau) d\tau$. Thus, $J_{IE} = \lim_{t \rightarrow \infty} x_3(t)$. Now, (21), (22), (23), (24), (33), and (34) yield the state space model of the overall system

$$\dot{x}(t) = F_{ex} x(t) + F_r r(t) = \begin{bmatrix} -a & a - K_a^* K_p & K_a^* K_i \\ a & -b & 0 \\ 0 & -1 & 0 \end{bmatrix} x(t) + \begin{bmatrix} 0 \\ 0 \\ 1 \end{bmatrix} r(t), \quad (35)$$

$$y(t) = F_{ey} x(t) = [0 \quad 1 \quad 0] x(t), \quad (36)$$

where $x(t) = [x_1(t) \quad x_2(t) \quad x_3(t)]^T$. Application of the Laplace transform to (35) and (36), with zero initial conditions, gives

$$X(s) = (sI - F_{ex})^{-1} F_r R(s), \quad (37)$$

Now, from (35) and (37) follows

$$X_3(s) = \frac{s^2 + s(a+b) + (ab - a^2 + K_p^*)}{\det(sI - F_{ex})} R(s) = \frac{s^2 + s(a+b) + (ab - a^2 + K_p^*)}{s^3 + s^2(a+b) + s(ab - a^2 + K_p^*) + K_i^*} R(s), \quad (38)$$

where $R(s) = \mathcal{L}[r(t)]$, $K_i^* = aK_a^*K_i$, $K_p^* = aK_a^*K_p$, $\det(\cdot)$ denotes determinant of a matrix, and $\det(sI - F_{ex}) = f(s)$ is a characteristic polynomial of the system. If the reference signal is $r(t) = R_0 h(t)$ and roots of $f(s)$ are $\sigma_1, \sigma_2, \sigma_3 < 0$, then, according to the limit theorem of the Laplace transform, $\lim_{t \rightarrow \infty} x_3(t) = \lim_{s \rightarrow 0} sX_3(s)$. Now, from (38) it follows $J_{IE} = [(ab - a^2 + K_p^*)/K_i^*] R_0$. Optimization procedure should yield K_p^* and K_i^* , i. e. K_p and K_i , that minimizes the value of J . In other words, design of the PI controller must provide $\min_{K_p, K_i} J_{IE}$, or $\max_{K_p, K_i} [K_i^*/(ab - a^2 + K_p^*)]$. As $\sigma_1, \sigma_2, \sigma_3 < 0$ are roots of $f(s)$, from (38) it follows that $\sigma_1 + \sigma_2 + \sigma_3 = a + b = p$, $\sigma_1\sigma_2 + \sigma_1\sigma_3 + \sigma_2\sigma_3 = ab - a^2 + K_p^*$, and $\sigma_1\sigma_2\sigma_3 = K_i^*$. Thus, optimization task becomes search for the maximum of $\sigma_1\sigma_2\sigma_3/(\sigma_1\sigma_2 + \sigma_1\sigma_3 + \sigma_2\sigma_3)$. According to [21], harmonic mean of the set $\sigma = \{\sigma_1, \sigma_2, \sigma_3\}$ is defined as

$$H(\sigma) = 3/[1/\sigma_1 + 1/\sigma_2 + 1/\sigma_3] = 3\sigma_1\sigma_2\sigma_3/(\sigma_1\sigma_2 + \sigma_1\sigma_3 + \sigma_2\sigma_3), \quad (39)$$

and arithmetic mean is defined as

$$A(\sigma) = (\sigma_1 + \sigma_2 + \sigma_3)/3. \quad (40)$$

Optimization procedure should yield maximum of the harmonic mean (39). The following relationship among harmonic and arithmetic means holds [21]

$$H(\sigma) \leq A(\sigma). \quad (41)$$

As $\sigma_1 + \sigma_2 + \sigma_3 = a + b = p$, regarding the problem at hand, $A(\sigma) = p/3$. Therefore, $H(\sigma) \leq p/3$, and $H(\sigma)$ will reach maximum value when $\sigma_1 = \sigma_2 = \sigma_3 = p/3$, as, in that case, $H(\sigma) = 3(p/3)^3/(3p^2/9) = p/3$. Thus, optimization procedure yields $K_i^* = p^3/27 = (a+b)^3/27$ and $K_p^* = a^2 - ab + p^2/3 = [(a+b)^2 - 3(ab - a^2)]/3$. Now, with (28), (29), and (30), optimal values are

$$K_i = -(p_1 + p_2)^3/(27K), \quad (42)$$

$$K_p = [(p_1 + p_2)^2 - 3p_1p_2]/(3K). \quad (43)$$

It is worth noting that the optimal PI controller provides transfer function of the overall system with triple negative real pole and without finite zeros. The transfer function models system locally, in vicinity of the steady state. Thus, optimization procedure yields a stable system, with aperiodic step response. Further, the integral action of the PI controller is placed in direct path of the system, thus the system will follow

constant reference signal without error in the steady state. Also, it is obvious from the performed analysis that $e_\infty = \lim_{t \rightarrow \infty} e(t) = \lim_{s \rightarrow 0} sE(s) = 0$.

Obtained placement of the system poles in the complex plane provides the fastest system step response. From (29) and (38), it is obvious that sum of the system poles equals $-(p_1 + p_2)$. Therefore, if one pole is moved away from the imaginary axis of the complex plane, to speed up the step response, the other two poles must come closer to the imaginary axis, thus becoming dominant and, consequently, slowing down the step response.

IV. EXPERIMENTAL ANALYSIS

To analyze performance of the optimal PI controller and verify obtained results, experiments were taken on the laboratory setup DTS 200 [8], presented in Fig. 3.

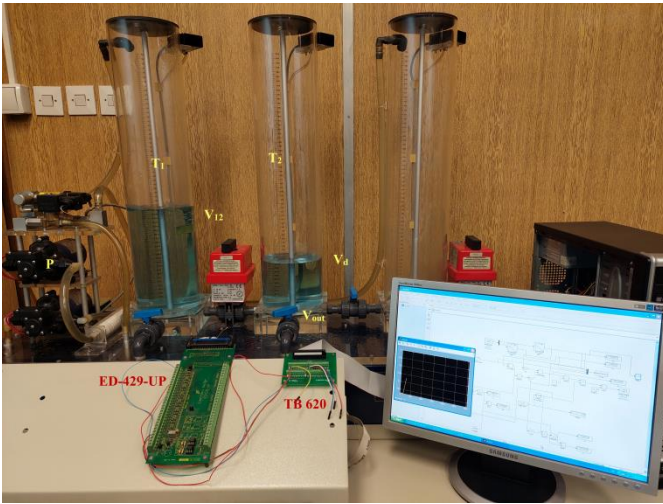


Fig. 3. The DTS 200 laboratory setup with connecting panels TB 620 and ED-429-UP, and PC

Valves in the system are set up, so the resulting system is the two-tank system, given in Fig. 1. Data acquisition and control application is realized by multifunction I/O card MF 634 [20] placed in a personal computer equipped with Windows operating system, Simulink software package, Simulink Desktop Real-Time toolbox, and MATLAB software package. The MF 634 I/O card is placed in a PCI Express slot of the personal computer. Also, the MF 634 card is connected to TB 620 terminal board, Fig. 3., via flat cable and 37 pin connector. The function of the TB 620 terminal board is to ease connection of the laboratory setup with the MF 634 I/O card. Further, the DTS 200 I/O signals are routed via flat cable and 50 pin connectors to ED-429-UP connecting panel, Fig. 3. Finally, the DTS 200 is connected to the MF 634 I/O card by proper wiring of inputs and outputs on the ED-429-UP connecting panel and the TB 620 terminal board. Sample application for data acquisition and control of the DTS 200 laboratory setup is given in Fig. 4. The sampling period was chosen according to recommendations [22], [11] and a priori knowledge of the

DTS200 [8], [9], [17]. Thus, sampling period was set to $T_s = 1$ s. To assess performance of applied controllers, average power of the error signal, denoted by J_e , and average power of the control signal, denoted by J_u , were chosen as performance measure indices.

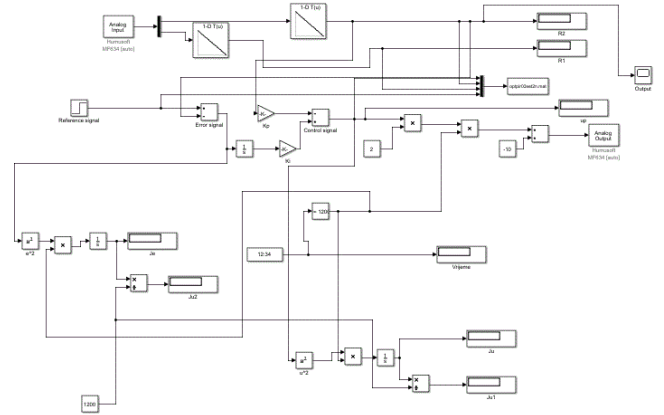


Fig. 4. Sample application for data acquisition and control of the DTS 200 laboratory setup

A. System identification

System identification experiments were carried out to obtain models of the system in certain steady states. Also, system identification yielded static characteristics of the water level sensors and static characteristics of the pump, i. e. actuator. Static characteristics of the water level sensors are given as sets of 61 pairs (sensor output voltage, water level). They were implemented in the data acquisition and control application as lookup tables, using Simulink blocks “1-D Lookup Table”. It should be noted that the input voltage range of the MF 634 I/O card is $[-10 \text{ V}, 10 \text{ V}]$ and output voltages of the water level sensors are slightly above 10 V when tanks are empty. Thus, data acquisition gives inaccurate water level readings at the beginning of the system operation. However, this fact does not influence the operation of the system and performance of implemented PI controllers.

The static characteristic of the pump consists of 12 pairs (input voltage, mass flow) and it is given in Fig. 5. From Fig. 5., it is obvious that the pump has a dead zone of approximately 2 V, and it saturates at 10 V. The static characteristic of the pump is almost linear in the range $[2 \text{ V}, 8 \text{ V}]$. Slope of the static characteristic of the pump, K_a , determines model of the pump, given by (7). In nonlinear model of the system given by (8) and (9), and all models derived from this one, appears modified slope, i. e. $K_a^* = K_a/(\rho S)$. Value of the K_a was determined from the static characteristic and its value is $K_a = 0.011131505 \text{ kg}/(\text{Vs})$, water density at approximately 20 °C is $\rho = 997 \text{ kg}/\text{m}^3$, and surface of the tank cross-section is $S = 0.0154 \text{ m}^2$. Thus, $K_a^* = 0.000725 \text{ m}/\text{s}$.

Further, to determine linearized models in the form of the transfer function $G_{tts}(s)$, given by (28) and (30), the two-tank system was driven by the signals $u_{in,1}(t) = 5h(t) + 0.4h(t - 2500)$ and $u_{in,2}(t) = 5.5h(t) + 0.4h(t - 2500)$, $h(t)$

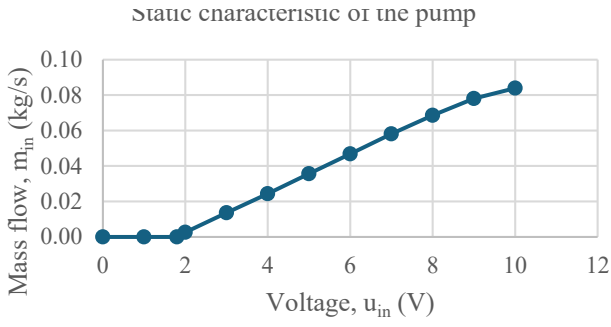


Fig. 5. Static characteristic of the pump, represents relationship between mass flow at the output of the pump and the pump input voltage, in the steady state

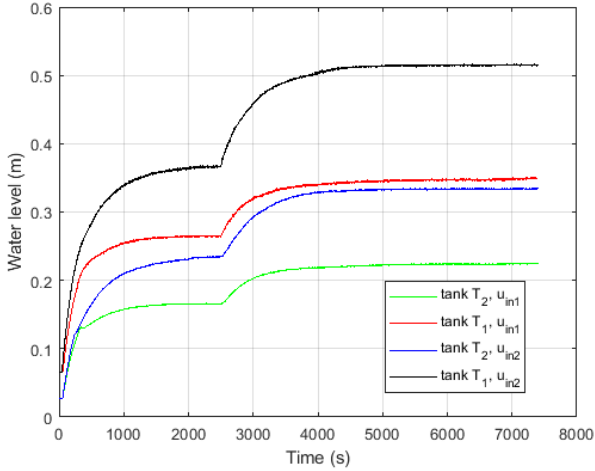


Fig. 6. The results of the system identification experiment, responses of the two-tank system to $u_{in,1}(t)$ and $u_{in,2}(t)$

denotes Heaviside step signal, in two different system identification experiments. The duration of each experiment was 7400 s. Thus, information on four different steady states were obtained. Due to construction of the DTS 200 laboratory setup, water in tanks waves during operation of the DTS 200. Thus, water level signals appear noisy. To assess value of the water levels in the steady states, values of the last 100 measurements were averaged, thus yielding values of $H_{1,SS}$ and $H_{2,SS}$. Responses of the two-tank system to $u_{in,1}(t)$ and $u_{in,2}(t)$ are given in Fig. 6. Summary of the system identification experiments is given in Table I. Table I, also, provides optimal values of the PI controller for different linearized models. This is done for easier future reference.

Actuation of the two-tank system with signal $0.4h(t - 2500)$, when the system is in the steady state, is part of the Ziegler-Nichols open loop experiment. The Ziegler-Nichols open loop experiment yields values of the parameters of PI controller to be used for performance assessment of the optimal PI controller. Two sets of parameters of the PI controller were computed based on the system models determined from the Ziegler-Nichols open loop experiments [10], [11].

These sets are $\{K_{pZN1} = 16.9839, K_{iZN1} = 0.16436\}$ and $\{K_{pZN2} = 11.3684, K_{iZN2} = 0.0898\}$. The first set of parameters has yielded a huge overshoot in the response of the system to $r(t) = 0.3h(t)$. In addition, and what is the problem,

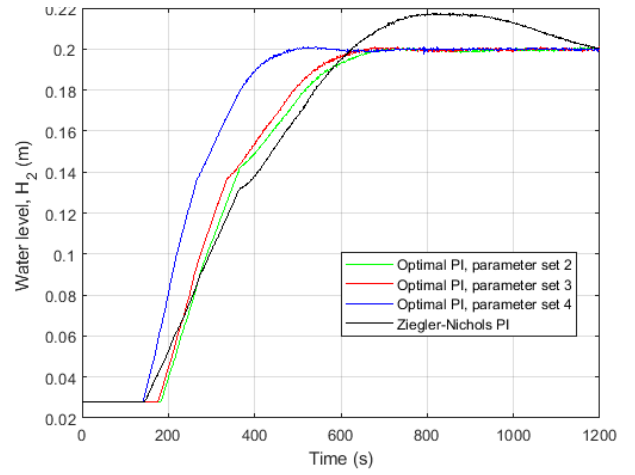


Fig. 7. The results of the step response experiment, system response to the reference signal $r(t)=0.2h(t)$

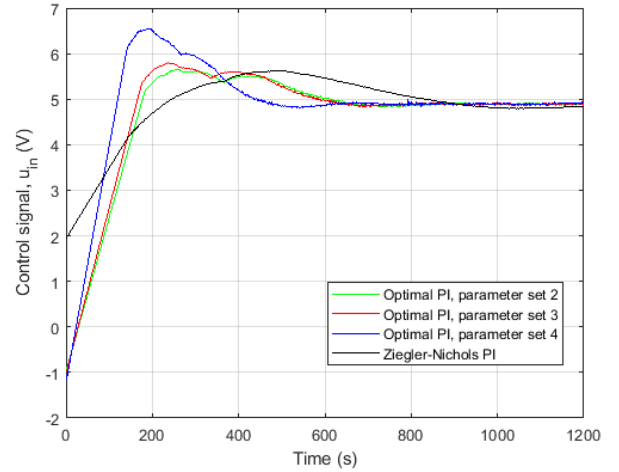


Fig. 8. The results of the step response experiment, control signal for the reference signal $r(t)=0.2h(t)$

the water level has reached the operational limit, i. e. 0.6 m, in the first tank. Therefore, the second set of parameters were adopted for use in the experimental analysis.

B. Step response

Step response experiments were performed for the two step type reference signals, i. e. $r(t) = 0.2h(t)$ and $r(t) = 0.3h(t)$. Duration of the experiments was $T = 1200$ s. The optimal PI controller was tested with three sets of parameters values, those given in rows 2., 3., and 4. in Table I. Summary of the experiments was given in Table II.

Fig. 7. and Fig. 8. give system outputs and control signals, respectively, for $r(t) = 0.2h(t)$. Fig. 9. and Fig. 10. give system outputs and control signals, respectively, in case of $r(t) = 0.3h(t)$. Optimal PI controller outperforms PI controller tuned according to the Ziegler-Nichols procedure, when reference signal $r(t) = 0.3h(t)$ was applied. When reference signal was $r(t) = 0.2h(t)$, the PI controller tuned according to the Ziegler-Nichols procedure was as accurate as the worst of optimally tuned PI controllers, but with larger control effort and 8.87% overshoot.

TABLE I
SUMMARY OF THE SYSTEM IDENTIFICATION EXPERIMENTS WITH PARAMETERS OF OPTIMALLY TUNED PI CONTROLLER

No.	Steady state			Transfer function parameters			Transfer function poles		Optimal PI controller parameters	
	Input voltage		Water level	a	b	K	p ₁	p ₂	K _p	K _i
	u _{in ss}	H _{1 ss}	H _{2 ss}							
1.	5.9 V	0.5153 m	0.3340 m	0.01179675	0.01820019	8.55264e-06	-0.00277496	-0.02722198	26.23738	0.116887
2.	5.5 V	0.3666 m	0.2344 m	0.01508132	0.02358708	1.0934e-05	-0.00366470	-0.03500369	33.85205	0.195852
3.	5.4 V	0.3491 m	0.2247 m	0.01573553	0.02444715	1.14083e-05	-0.00376406	-0.03641862	35.16171	0.210636
4.	5.0 V	0.2646 m	0.1659 m	0.01836373	0.02928898	1.33137e-05	-0.00466737	-0.04298534	41.78391	0.301023

TABLE II
SUMMARY OF THE STEP RESPONSE EXPERIMENTS
FOR THE SYSTEM WITH OPTIMALLY TUNED PI CONTROLLER AND
PI CONTROLLER TUNED ACCORDING TO THE ZIEGLER-NICHOLS PROCEDURE

PI controller parameters		Reference signal, r(t) (m)	Performance measure indices		Note
K _p	K _i		J _e	J _u	
33.85205	0.195852	0.3	1.4429e-2	3.3838e+1	Optimal
35.16171	0.210636	0.3	1.3748e-2	3.4150e+1	Optimal
41.78391	0.301023	0.3	1.1244e-2	3.6602e+1	Optimal, overshoot 5.67%
11.3684	0.0898	0.3	1.4421e-1	3.7201e+1	Ziegler-Nichols
33.85205	0.195852	0.2	6.8243e-3	2.3370e+1	Optimal
35.16171	0.210636	0.2	6.5188e-3	2.3776e+1	Optimal
41.78391	0.301023	0.2	5.1700e-3	2.5115e+1	Optimal
11.3684	0.0898	0.2	6.8231e-3	2.4281e+1	Ziegler-Nichols overshoot 8.87%

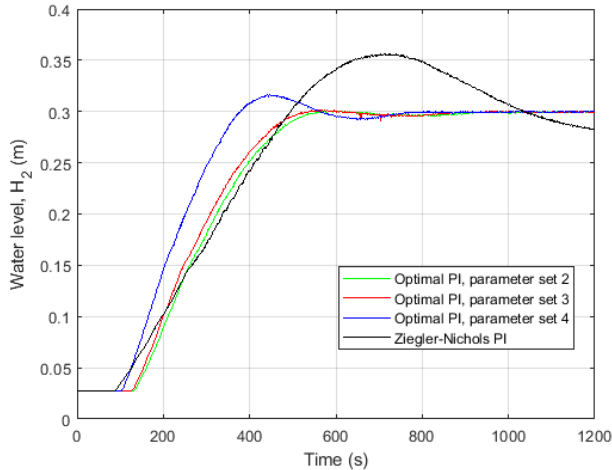


Fig. 9. The results of the step response experiment, system response to the reference signal $r(t)=0.3h(t)$

In addition, performance of the PI controller tuned with the Ziegler-Nichols method, with proportional term placed in the feedback path, was tested. In the case $r(t) = 0.2h(t)$, values of the performance indices measures were $J_e = 1.0573e - 2$ and $J_u = 2.1627e + 1$. This is a significant deterioration of the controller performance when compared to one with proportional term placed in the direct path. Further, in the case $r(t) = 0.3h(t)$, values of the performance indices measures were $J_e = 2.1648e - 2$ and $J_u = 3.1244e + 1$. This presents improvement when compared to the PI controller with proportional term placed in the direct path. However, this yields

a significantly less accurate system than the one equipped with the optimal PI controller, while control efforts were comparable. Also, during operation the system has approached near the limit in the first tank, i. e. the water level was approximately 0.53 m.

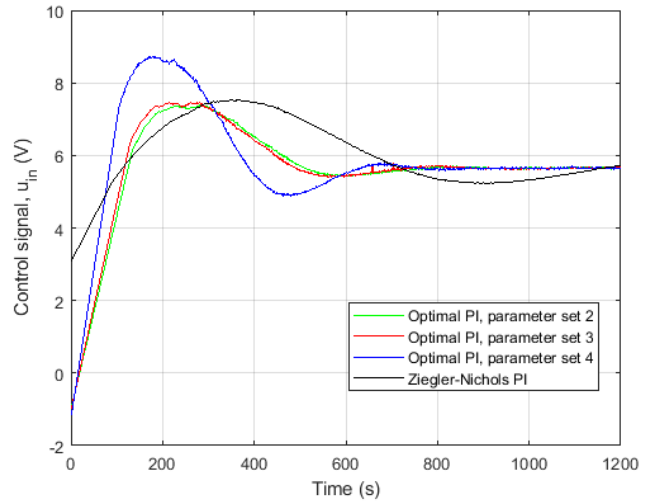


Fig. 10. The results of the step response experiment, control signal for the reference signal $r(t)=0.3h(t)$

C. Reference tracking

Reference tracking experiments were organized as tracking of a piecewise constant reference signal. Duration of the experiments was $T = 3600$ s. Optimally tuned PI controller, with the third set of parameters, was applied in the task of reference tracking, as well as PI controller tuned according to the Ziegler-Nichols procedure.

Reference signal was $r(t) = 0.25h(t) + 0.05h(t - 1000) - 0.07h(t - 1500) + 0.02h(t - 2500) - 0.03h(t - 3000)$. Results of the experiment were summarized in Table III. Fig. 11. and Fig. 12. give system outputs and control signals, respectively. It is obvious that optimally tuned PI controller tracks reference signal more accurately and with less control effort when compared to the PI controller tuned according to the Ziegler-Nichols procedure.

Also, performance of the PI controller tuned with the Ziegler-Nichols method, with proportional term placed in the feedback path, was tested in the reference tracking task. Values of the performance indices measures were $J_e = 5.6584e - 3$ and $J_u = 2.7013e + 1$. This presents a significant deterioration of tracking accuracy when compared to the system with implemented the other tested controllers.

TABLE III
SUMMARY OF THE REFERENCE TRACKING EXPERIMENTS FOR THE
SYSTEM WITH OPTIMALLY TUNED PI CONTROLLER AND PI CONTROLLER
TUNED ACCORDING TO THE ZIEGLER-NICHOLS PROCEDURE

PI controller parameters		Performance measure indices		Note
K_p	K_i	J_e	J_u	
11.3684	0.0898	3.6634e-3	3.0058e+1	Ziegler-Nichols
35.16171	0.210636	3.6510e-3	2.8307e+1	Optimal

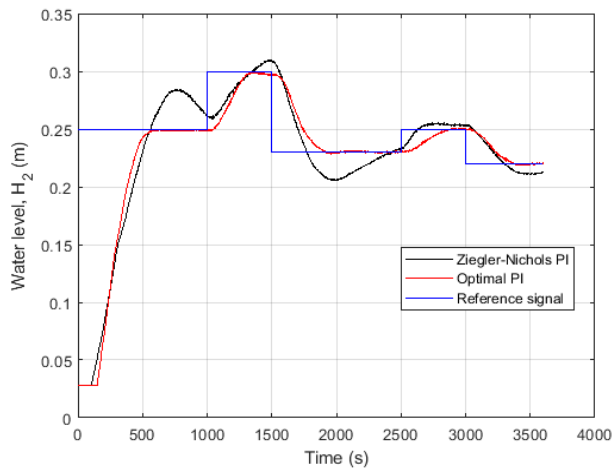


Fig. 11. The results of the reference tracking experiment, system outputs for the piecewise constant reference signal

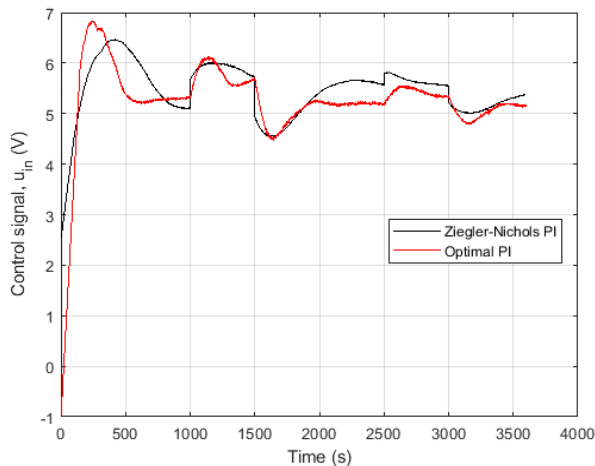


Fig. 12. The results of the reference tracking experiment, control signals for the piecewise constant reference signal

D. Comparison with a PID controller

An additional set of experiments has been performed utilizing the PID controller to control the two-tank system. The PID controller was tuned according to the Ziegler-Nichols method which yielded the following set of parameters $K_p = 15.15787$, $K_i = 0.1996$, and $K_d = 287.84$. Initial experiments revealed that the differential gain must be lowered, and the differential term of the controller must include a filter to yield adequate performance of the system. The reason for this is the presence of the noise in the system output signal. Physical

explanations rely on the construction of the DTS200 system, i. e. water inflow in a tank produces wavy water surface that appears as a noise in the output of the system. The differential part of the controller, without the filter, and the noise produce noticeable ripples in the control signal. Therefore, transfer function of the applied PID controller was $G_{PID}(s) = K_p + K_i s^{-1} + K_d [N/(1 + Ns^{-1})]$, where K_d denotes differential gain and N denotes filter coefficient. Further, fine tuning of the PID controller was iteratively performed to obtain an applicable controller. Additional tuning significantly affected the value of the differential gain, i. e. it was set to $K_d = 10$. Also, value of the filter coefficient was set to $N = 10$. The step response experiment for $r(t) = 0.3h(t)$ has had to be interrupted due to safety reasons. More precise, the water level in the first tank was over 0.58 m, thus almost reached the limit. In the case $r(t) = 0.2h(t)$ the values of the performance measure indices were $J_e = 4.6370e - 3$ and $J_u = 3.0868e + 1$, but the overshoot was greater than 25%. These results yielded reduced value of the integral gain, i. e. $K_i = 0.1$. This change yielded $J_e = 6.1958e - 3$ and $J_u = 2.7765e + 1$ for the step response with $r(t) = 0.2h(t)$ and $J_e = 1.1138e - 2$ and $J_u = 3.8535e + 1$ for the step response with $r(t) = 0.3h(t)$. Thus, the system was slightly more accurate with increased control effort. However, in the case of $r(t) = 0.3h(t)$ the overshoot was more than 10% and water level in the first tank was more than 0.51 m. The reference tracking experiments yielded $J_e = 3.2746e - 3$ and $J_u = 3.0829e + 1$. Hence, significant overshoot was present in the system output every time the reference signal exhibited a step change. Thus, the performance of the system significantly deteriorated.

E. Disturbance rejection

To assess disturbance rejection capability of the optimal PI controller, step response experiments were performed with $r(t) = 0.25h(t)$. Disturbance to the system operation was partial opening of the valve V_d , Fig. 3., at time instant $t = 1000$ s. Opening of the valve V_d results in an increase of water flow out of the tank T_2 . The valve V_d was closed at time instant $t = 2000$ s, thus reducing the water flow out of the tank T_2 . Duration of the experiment was $T = 3000$ s. Optimally tuned PI controller with the third set of parameters was applied in the experiment. Fig. 13. and Fig. 14. give system output and control signal, respectively. The controller was successful in disturbance rejection task and its performance measure indices were $J_e = 4.1397e - 3$ and $J_u = 3.5124e + 1$.

V. FEEDFORWARD MODIFICATION OF THE CONTROLLER

Due to the structure of the PI controller, proportional action is placed in the feedback path, implemented optimization procedure, and very slow dynamics of the two-tank system, the system starts slowly at the beginning of the operation. This appears as a dead time of the system. During that period, the pump operates on the border line between a dead zone and a regular operation, which might deteriorate future performance and life expectancy of the pump.

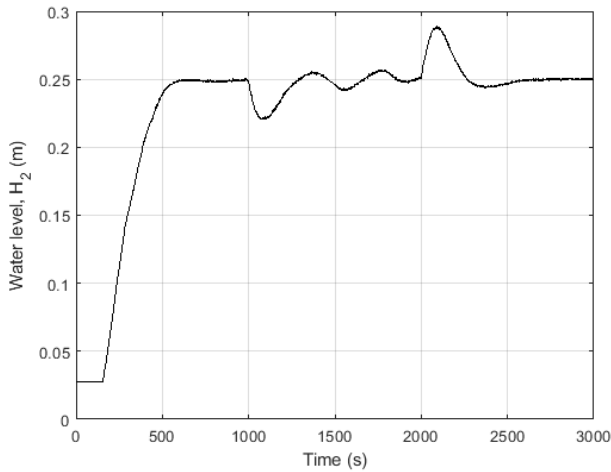


Fig. 13. The results of the disturbance rejection experiment, system output for the reference signal $r(t)=0.25h(t)$, while disturbance was valve V_d opening at $t=1000$ s and valve V_d closing at $t=2000$ s

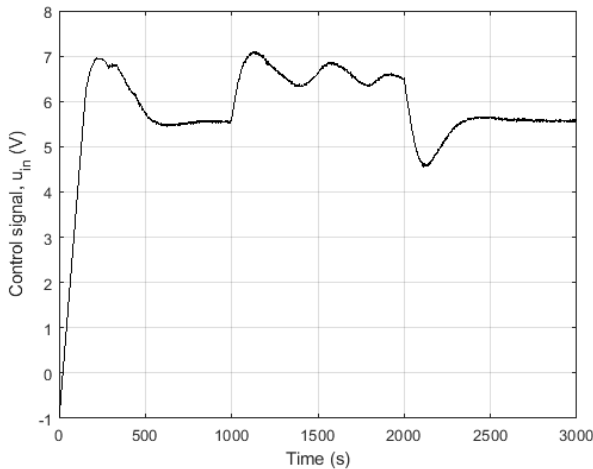


Fig. 14. The results of the disturbance rejection experiment, control signal for the reference signal $r(t)=0.25h(t)$, while disturbance was valve V_d opening at $t=1000$ s and valve V_d closing at $t=2000$ s

At the beginning of operation, parallel PI controller, i.e. controller with the proportional part in the direct path of the system, usually, exhibits fast response to a step change in a reference signal. It is easy to explain this fact, reference signal step change results in a step change of an error signal. Consequently, the value of a control signal, dominantly determined by the proportional part of the controller at the beginning of the operation, has significant change. Thus, the operating point of the pump moves towards saturation region and pump provides significant power to the system. Therefore, the idea is to modify the structure of the system to have parallel PI controller at the beginning of system operation and to have structure given in Fig. 2. at the later stages of the system operation, i.e. as time advances. The modified structure of the system is provided in Fig. 15. The structure of the system includes a feedforward part [23] with a time varying gain, $K_{ff} = K_p \exp(-t/\tau)h(t)$, where K_p is proportional gain of the optimal PI controller, τ is the time constant, in this case a design parameter, and $h(t)$ is introduced due to causality of the system. It is obvious that K_{ff} has significant values at the beginning of

system operation, while its value reduces towards zero as time advances and value of the parameter t increases. One should expect that the system will be detuned, and its overall performance will not be optimal. However, after certain amount of time, value of K_{ff} will become insignificant, i.e. neglectable, and the system should operate as designed. Furthermore, at the beginning of the system operation, the pump will operate away from the dead zone, and the response of the system will be faster when compared to the response of the original system, with the structure given in Fig. 2.

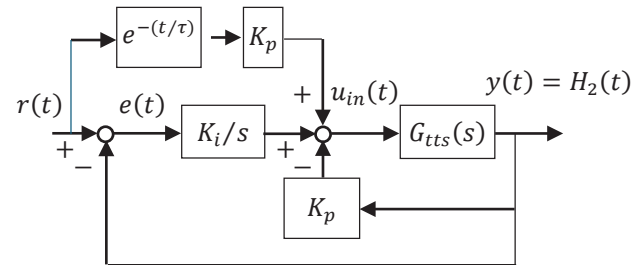


Fig. 15. Block diagram of the system with optimally tuned PI controller and the feedforward modification

To evaluate the idea of the feedforward modification of the system structure, experiments on the two-tank system were performed. The first experiment provides step responses of the system for different step reference signals and different values of the time constant τ . The outputs of the system, for the reference signal $r(t) = 0.2h(t)$ (m), are given in Fig. 16., while control signals are given in Fig. 17. Further, the outputs of the system, for the reference signal $r(t) = 0.3h(t)$ (m), are given in Fig. 18., while control signals are given in Fig. 19. Summary of the first experiment, with performance measure indices, is given in Table IV. The second experiment analyses reference tracking capabilities of the modified system. The output of the modified system and output of the optimal system are given in Fig. 20., while control signals are provided in Fig. 21. The performance measure indices for the second experiment are given in Table V.

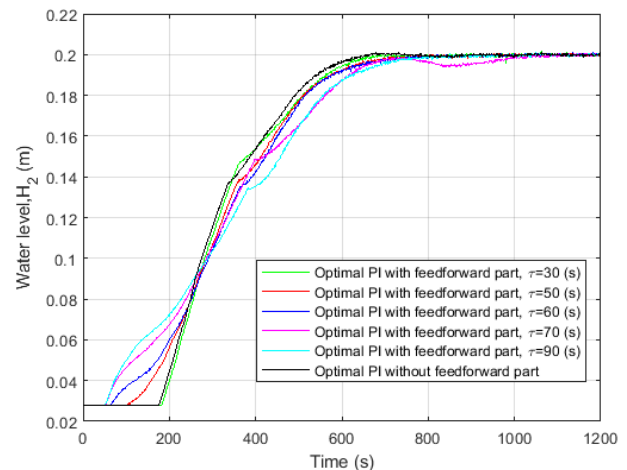


Fig. 16. Comparison of the optimally tuned PI controller and the controller with the feedforward modification. The results of the step response experiment, system response to the reference signal $r(t)=0.2h(t)$

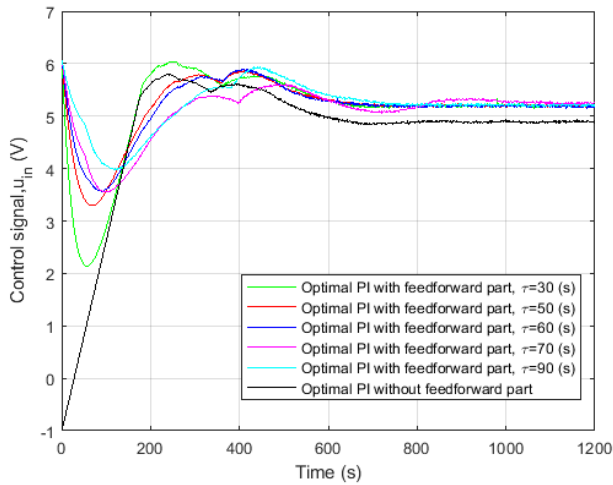


Fig. 17. Comparison of the optimally tuned PI controller and the controller with the feedforward modification. The results of the step response experiment, control signal for the reference signal $r(t)=0.2h(t)$

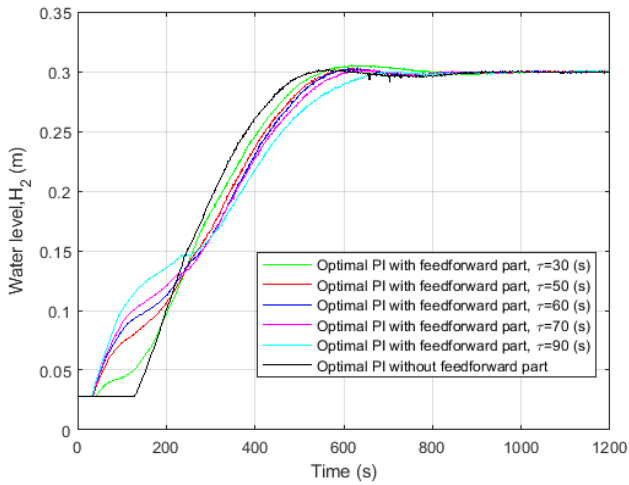


Fig. 18. Comparison of the optimally tuned PI controller and the controller with the feedforward modification. The results of the step response experiment, system response to the reference signal $r(t)=0.3h(t)$

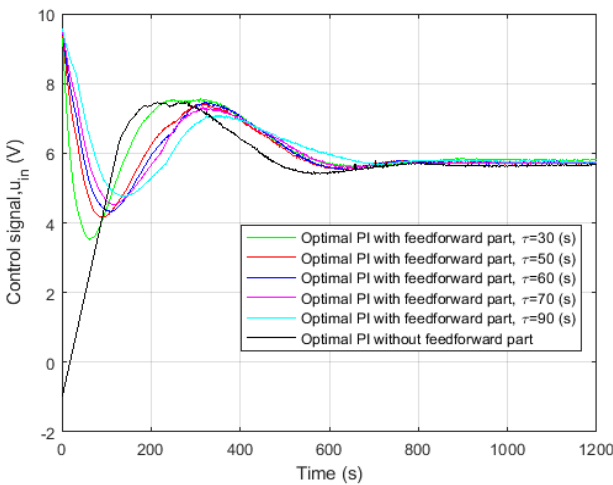


Fig. 19. Comparison of the optimally tuned PI controller and the controller with the feedforward modification. The results of the step response experiment, control signal for the reference signal $r(t)=0.3h(t)$

TABLE IV
SUMMARY OF THE STEP RESPONSE EXPERIMENTS
FOR THE SYSTEM WITH OPTIMALLY TUNED PI CONTROLLER AND
OPTIMAL PI CONTROLLER WITH THE FEEDFORWARD MODIFICATION

PI controller parameters	FF mod.	Reference signal, $r(t)$ (m)	Performance measure indices		Note
			J_e	J_u	
K_p	K_i	τ (s)			
35.16171	0.210636	30	0.3	1.3447e-2 3.7499e+1	With ff mod.
35.16171	0.210636	50	0.3	1.2343e-2 3.6264e+1	With ff mod.
35.16171	0.210636	60	0.3	1.2003e-2 3.6518e+1	With ff mod.
35.16171	0.210636	70	0.3	1.1702e-2 3.6719e+1	With ff mod.
35.16171	0.210636	90	0.3	1.1057e-2 3.7274e+1	With ff mod.
35.16171	0.210636	none	0.3	1.3748e-2 3.4150e+1	Optimal
35.16171	0.210636	30	0.2	6.6724e-3 2.6986e+1	With ff mod.
35.16171	0.210636	50	0.2	6.3952e-3 2.7069e+1	With ff mod.
35.16171	0.210636	60	0.2	6.2188e-3 2.7025e+1	With ff mod.
35.16171	0.210636	70	0.2	5.8137e-3 2.6176e+1	With ff mod.
35.16171	0.210636	90	0.2	5.7513e-3 2.7293e+1	With ff mod.
35.16171	0.210636	none	0.2	6.5188e-3 2.3776e+1	Optimal

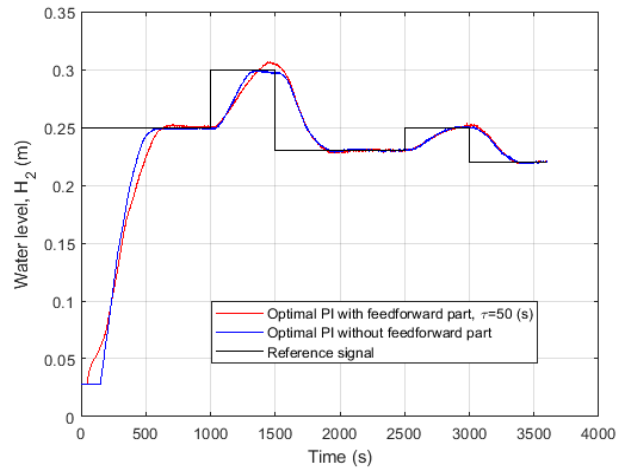


Fig. 20. Comparison of the optimally tuned PI controller and the controller with the feedforward modification. The results of the reference tracking experiment, system outputs for the piecewise constant reference signal

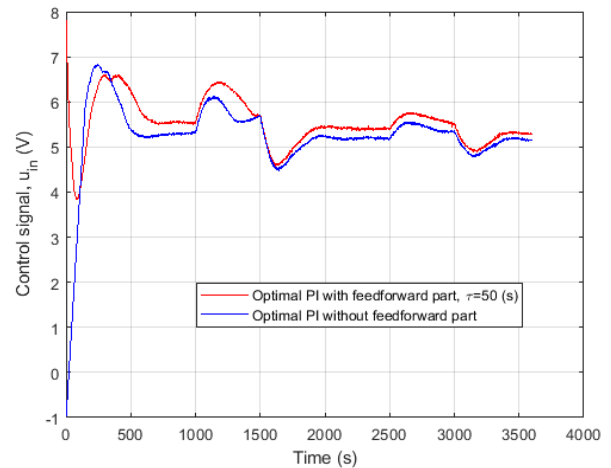


Fig. 21. Comparison of the optimally tuned PI controller and the controller with the feedforward modification. The results of the reference tracking experiment, control signals for the piecewise constant reference signal

TABLE V
SUMMARY OF THE REFERENCE TRACKING EXPERIMENTS FOR THE
SYSTEM WITH OPTIMALLY TUNED PI CONTROLLER AND PI CONTROLLER
WITH THE FEEDFORWARD MODIFICATION

PI controller parameters		Feedforward modification	Performance measure indices		Note
K_p	K_i	τ (s)	J_e	J_u	
35.16171	0.210636	50	3.4656e-3	3.0981e+1	With feedforward modification
35.16171	0.210636	none	3.6510e-3	2.8307e+1	Optimal

VI. CONCLUSIONS

The newly proposed optimal PI controller for a coupled tanks system was experimentally tested. The tests have been performed on the DTS 200 laboratory setup, properly configured as the two-tank system by positioning system valves. As optimal PI controller operates on linear model, i. e. transfer function of the system, therefore several local linear models have been identified. Local linear models, i. e. transfer functions, have been computed based on the steady state data and the derived mathematical model of the two-tank system. Steady state data has been fitted into the intended operating region of the system.

Experiments have been organized as system step response experiments, reference tracking experiments, and disturbance rejection experiments. Performed experiments have verified designed performance of the optimal PI controller, as it has provided aperiodic step response, approximately three times faster than response obtained in the open loop experiments. When overshoot appeared in the step response, due to modelling errors, it was approximately 5%. It is important to note that in the performed experiments, the water level in the first tank, tank T_1 , has had a significant margin with respect to operational limit, i.e. water level of 0.6 m.

Analyzed optimal PI controller has been tracking piecewise constant reference signal successfully. Its performance was better than the PI controller tuned according to the Ziegler-Nichols procedure, regardless of whether the proportional gain was in the direct or in the feedback path. It is worth noting that the optimal PI controller has been successfully tracking negative step changes in the reference signal, i. e. reference tracking has been fast without undershoot.

Disturbance of the system operation has been performed as output valve opening and closing. Optimal PI controller has successfully eliminated disturbance in the output signal, with acceptable dynamics.

Also, performance of the optimal PI controller was compared to the performance of the PID controller tuned with the Ziegler-Nichols procedure. Filter in the differential part of the PID controller appeared to be a necessity. Further, it turns out that the PID controller requires fine tuning, which yields significantly lowered values of the differential and integral gain. These features of the PID controller have provided safe operation of the system, values of the performance measure indices similar to ones obtained with the optimal PI controller, and with the significant overshoot.

Optimal PI controller has exhibited a slow start at the beginning of system operation, i. e. when tanks were empty. In addition, the actuator operates near the dead zone in that case. To remedy the situation, the feedforward modification with the time varying gain has been introduced. Experimental analysis of the modified control structure has been performed. Step response and reference tracking experiments, carried out on the testbed DTS 200, have justified application of the modified control structure.

Future work should provide theoretically tractable and easy to implement solutions. Also, migration of the optimal PI controller and the proposed modification to a standard industrial platform, based on a programmable logic controller, might appear as a challenge.

REFERENCES

- [1] A. L. Reis, M. A.R. Lopes, A. Andrade-Campos, and C. Henggeler Antunes, "A review of operational control strategies in water supply systems for energy and cost efficiency," *Renewable and Sustainable Energy Reviews*, vol. 175, 2023, 113140, ISSN 1364-0321, <https://doi.org/10.1016/j.rser.2022.113140>. (<https://www.sciencedirect.com/science/article/pii/S1364032122010218>)
- [2] S. C. Olisa, C. N. Asiegbu, J. E. Olisa, B. O. Ekengwu, A. A. Shittu, and M. C. Eze, "Smart two-tank water quality and level detection system via IoT," *Heliyon*, vol. 7, issue 8, 2021, e07651, ISSN 2405-8440, <https://doi.org/10.1016/j.heliyon.2021.e07651>. (<https://www.sciencedirect.com/science/article/pii/S2405844021017540>)
- [3] G. Hendrickson and L. Sela, "Optimizing equity in intermittent water supply systems: A volume-driven demand and flow control approach," *Sustainable Cities and Society*, vol. 112, 2024, 105615, ISSN 2210-6707, <https://doi.org/10.1016/j.scs.2024.105615>. (<https://www.sciencedirect.com/science/article/pii/S2210670724004402>)
- [4] E. Creaco, A. Campisano, N. Fontana, G. Marini, P.R. Page, and T. Walski, "Real time control of water distribution networks: A state-of-the-art review," *Water Research*, vol. 161, pp. 517-530, 2019, ISSN 0043-1354, <https://doi.org/10.1016/j.watres.2019.06.025>. (<https://www.sciencedirect.com/science/article/pii/S0043135419305366>)
- [5] V. Kecman, *Dinamika procesa*, Sveučilište u Zagrebu, Zagreb, 1988.
- [6] J. Igić, M. Božić, P. Marić, and I. Krčmar, "Adaptive control based on internal model," in *Proceedings of the XLV ETRAN Conference*, Bukovička Banja, June 4 – 7, 2001. pp. 209 – 212.
- [7] J. Igić, M. Božić, and I. Krčmar, "An AIMNC for the Typical Industrial Processes," in *Proceedings of 2nd International Conference on Electrical, Electronic and Computing Engineering IcETRAN 2015*, Silver Lake, Serbia, June 8 – 11, 2015, ISBN 978-86-80509-71-6, pp. AUI3. 1. 1 – 7
- [8] DTS 200, Laboratory setup Three-Tank-System, Amira GmbH, Duisburg, Germany, May 2002.
- [9] M. Božić, P. Marić, I. Radojičić, I. Krčmar, and J. Igić, "An Analysis of dynamics of specific coupled tanks system," in *Proceedings of the XLVII ETRAN Conference*, vol. 1, Herceg Novi, June 8 – 13, 2003. pp. 328 – 331.
- [10] M. R. Stojić, *Digitalni sistemi upravljanja*, III izmenjeno i dopunjeno izdanje, Nauka, Beograd, 1994.
- [11] K. J. Åström and B. Wittenmark, *Adaptive control*, Addison-Wesley Publishing Company, 1989.
- [12] R. Vilanova and A. Visioli, *PID Control in the Third Millenium, Lessons Learned and New Approaches*, Advances in Industrial Control, Springer, 2012.
- [13] J.-H. Urrea-Quintero, J.-A. Hernández-Riveros, and N. Muñoz-Galeano, "Optimum PI/PID Controllers Tuning via an Evolutionary Algorithm," *PID Control for Industrial Processes*. InTech, Sep. 12, 2018. doi: 10.5772/intechopen.74297.
- [14] H. Du, X. Hu, J. Xiao, G. Zhang, and J. Liu, "Optimal PI controller design for second order plus time delay processes based on gain margin and improved error integration indices," in *Proc. 2018 13th IEEE Conference on Industrial Electronics and Applications (ICIEA)*, Wuhan, China, 2018, pp. 2607-2611, doi: 10.1109/ICIEA.2018.8398151.

- [15] S. Sengupta and C. Dey, "Auto-tuned Optimal PI Controllers for MIMO Processes," in *Proc. 2021 IEEE 4th International Conference on Computing, Power and Communication Technologies (GUCON)*, Kuala Lumpur, Malaysia, 2021, pp. 1-6, doi: 10.1109/GUCON50781.2021.9573839.
- [16] S. N. Vukosavić, *Digital Control of Electrical Drives*, Springer, 2007.
- [17] I. Krčmar, A. Rakić, V. Đalić, B. Derajić, and P. Marić, "Towards Optimal PI Controller for a Coupled Tanks System," in *Proc. 2024 11th International Conference on Electrical, Electronic and Computing Engineering (IcETRAN)*, Nis, Serbia, 2024, pp. 1-5, doi: 10.1109/IcETRAN62308.2024.10645196.
- [18] R. Marino and P. Tomei, *Nonlinear Control Design Geometric, Adaptive, and Robust*, Prentice Hall, 1995.
- [19] B. D. Kovačević, Ž. Đurović, S. Stanković, *Signali i sistemi*, Akademska misao, Beograd, 2008.
- [20] *MF 634 Multifunction I/O Card User's Manual*, Humusoft s. r. o., Praha, Czech Republic, 2014.
- [21] D. S. Mitrinović, P. M. Vasić, *Analitičke nejednakosti*, Izdavačko preduzeće "Građevinska knjiga" Beograd, 1970.
- [22] J. Igić, M. Božić, and P. Marić, "Neuro-Adaptive Control Based on Internal Model," in *Proc. XLVI ETRAN Conference*, Banja Vrucica – Teslic, June 4-7, 2002, vol. I, pp. 161-164.
- [23] K. J. Åström and T. Hägglund, *PID Controllers: Theory, Design, and Tuning*, 2nd edition, Instrument Society of America, 1995.